Carrier Protein-Free Enzymatic Biaryl Coupling in Arylomycin A2 Assembly and Structure of the Cytochrome P450 AryC**

Hülya Aldemir[+],[a, b] Shuangjie Shu[+],[a, b] Francoise Schaefers,[b] Hanna Hong,[b] René Richarz,[b] Sabrina Harteis,[b] Manuel Einsiedler,[a] Tobias M. Milzarek,[a] Sabine Schneider,*[c] and Tobias A. M. Gulder*[a, b]

This work is dedicated to Prof. Dr. Dr. h.c. mult. Gerhard Bringmann on the occasion of his 70th birthday.

Abstract: The arylomycin antibiotics are potent inhibitors of bacterial type I signal peptidase. These lipohexapeptides contain a biaryl structural motif reminiscent of glycopeptide antibiotics. We herein describe the functional and structural evaluation of AryC, the cytochrome P450 performing biaryl coupling in biosynthetic arylomycin assembly. Unlike its enzymatic counterparts in glycopeptide biosynthesis, AryC converts free substrates without the requirement of any protein interaction partner, likely enabled by a strongly hydrophobic cavity at the surface of AryC pointing to the substrate tunnel. This activity enables chemo-enzymatic assembly of arylomycin A2 that combines the advantages of liquid- and solid-phase peptide synthesis with late-stage enzymatic cross-coupling. The reactivity of AryC is unprecedented in cytochrome P450-mediated biaryl construction in non-ribosomal peptides, in which peptidyl carrier protein (PCP)-tethering so far was shown crucial both in vivo and in vitro.

[a] Dr. H. Aldemir,[+] S. Shu,[+] M. Einsiedler, Dr. T. M. Milzarek, Prof. T. A. M. Gulder
Chair of Technical Biochemistry
Technical University of Dresden
Bergstraße 66, 01069 Dresden (Germany)
E-mail: tobias.gulder@tu-dresden.de

[b] Dr. H. Aldemir,[+] S. Shu,[+] Dr. F. Schaefers, Dr. H. Hong, Dr. R. Richarz, Dr. S. Harteis, Prof. T. A. M. Gulder
Biosystems Chemistry, Faculty of Chemistry
Technical University of Munich
Lichtenbergstraße 4, 85748 Garching (Germany)

[c] Dr. S. Schneider
Department of Chemistry
Ludwig-Maximillians-University Munich
Butenandtstraße 5–13, 81377 Munich (Germany)
E-mail: sabine.schneider@cup.lmu.de

[+] These authors contributed equally to this work.

[**] A previous version of this manuscript has been deposited on a preprint server (https://doi.org/10.33774/chemrxiv-2021-t1817).

Supporting information for this article is available on the WWW under https://doi.org/10.1002/chem.202103389

Ever since their discovery, glycopeptides such as vancomycin (aglycon structure **1**, Figure 1) have fascinated researchers across disciplines.[1] Biosynthetically, their amino acid precursors are fused by non-ribosomal peptide synthetases (NRPS).[2] The resulting linear precursor peptide gets oxidatively cross-coupled by dedicated cytochrome P450 enzymes prior to its release from the terminal PCP of the NRPS.[3,4] In addition, a so-called X-domain is required to orchestrate enzymatic crosslinking.[5] This recent finding also set the stage for the first successful in vitro reconstitution of the entire oxidative cross-linking cascade to chemo-enzymatically prepare glycopeptide aglycons and modified analogs.[6] This large body of work conducted over decades not only ultimately established the biosynthetic logic of glycopeptide assembly,[7] but also revealed key challenges in applying the oxidative biosynthetic machinery in vitro as biocatalytic system. Most importantly, the necessity of equimolar amounts of both coenzyme A (for precursor activation allowing PCP tethering) and of PCP-X didomain protein as crucial template for substrate recognition by the cross-linking P450s precludes a truly (bio-)catalytic approach.

Another class of biaryl-containing peptides (BCPs) are the arylomycins, such as arylomycin A2 (**2**).[8] The arylomycins inhibit bacterial type I signal peptidase (SPase), an essential enzyme of the secretory pathway that is not addressed by any approved drug and thus represents a promising new antibiotic target.[9]

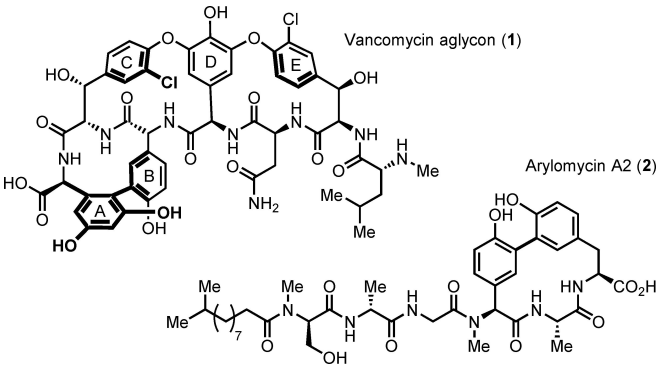

Figure 1. Structures of vancomycin aglycon (**1**) and arylomycin A2 (**2**).

Owing to these properties, the arylomycins have attracted strong interest from the synthetic community. The first total syntheses relied on the preparation of linear peptide precursors followed by macrocyclization by Suzuki-Miyaura reaction.[10–12] Further work provided elevated yields to the macrocyclic arylomycin core by macrolactamization[13] and improved Suzuki-Miyaura macrocyclization.[14] Romesberg and Baran enabled access to the macrocycle by C–H functionalization of the unmodified aromatic amino acids by copper-mediated oxidative phenol coupling.[15] This elegant approach, however, requires two equivalents of the copper reagent. Most recent work achieved catalytic oxidative cross-coupling using iron (tetraphenylporphyrinato) chloride (FeCl[TPP]), which in turn necessitates the application of removable *tert*-Butyl (^{t}Bu) activating groups at the phenolic residues.[16] Taken together, despite the tremendous developments in arylomycin synthesis, there is still no catalytic route available that employs non-activated aromatic amino acids, in analogy to the natural pathway.

The biosynthetic machinery of the arylomycins was discovered in 2011 by Moore, Dorrestein and coworkers, combining imaging mass spectrometry and genome mining.[17] They identified a NRPS composed of the three proteins AryA, AryB and AryD and proposed it to assemble a linear lipopeptide precursor **3** (cf. Scheme 1A). Similar to glycopeptide biosynthesis, **3** was thought to undergo oxidative macrocyclization by the pathway-specific cytochrome P450 AryC while still bound to the terminal PCP of the NRPS, prior to thioesterase-mediated hydrolytic release of the product, for example, arylomycin A2 (**2**).[18] Interestingly, the NRPS does not contain an X-domain, pointing at different preconditions for enzymatic cross-coupling in arylomycin versus glycopeptide biosynthesis. Within this work, we thus set out to probe the function of AryC as biaryl coupling enzyme in the assembly of **2**, thereby also shedding light on its requirements for protein interaction partners to function, and elucidated its X-ray crystal structure.

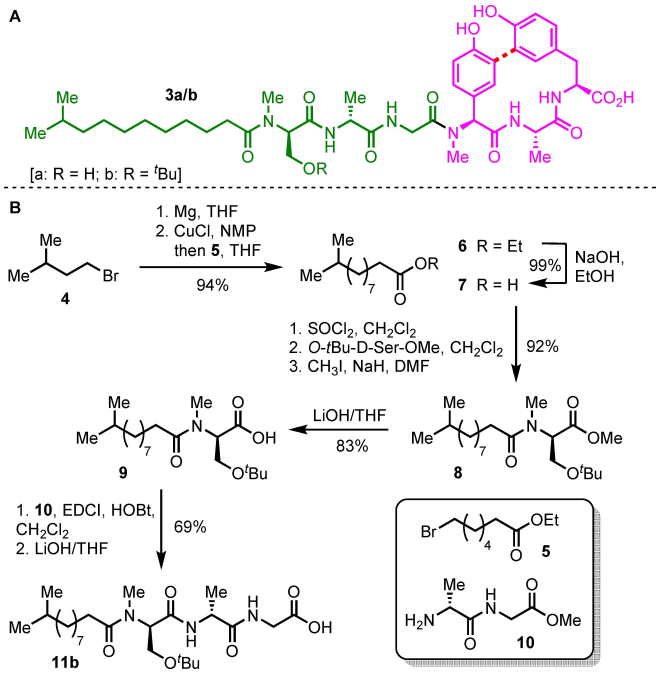

Scheme 1. A) Structure of the linear precursor peptide **3**. Parts to be assembled by LPPS shown in green, by SPPS shown in pink. Dotted red line indicates the site of the strategic biocatalytic cross-coupling reaction using AryC. B) LPPS synthesis of the lipopeptide side **11 b**.

Aiming for a convergent synthesis of the linear peptide precursor **3** while simultaneously avoiding peptide assembly and purification steps with the epimerization-prone hydroxyphenyl glycine (HPG) residue in place, the tripeptide portion (Scheme 1A, pink), ultimately composing the macrocycle of **2**, was to be prepared by solid-phase peptide synthesis (SPPS). The lipopeptide side-chain (Scheme 1A, green) was synthesized by liquid phase peptide synthesis (LPPS). Preparation of the Grignard reagent from 1-bromo-3-methylbutane (**4**) using activated Mg turnings in THF with subsequent cuprate formation and addition to ethyl 7-bromoheptanoate (**5**) delivered ester **6** in 94% yield (Scheme 1B).[19] Saponification of **6** with NaOH resulted in the required fatty acid building block **7** in 99% yield. Activation of **7** using $SOCl_2$ and direct application of the resulting acid chloride for acylation of *O*-^{t}Bu-D-serine methyl ester, followed by mono *N*-methylation of the amide gave ester **8** (combined 92% yield). Saponification of **8** in THF/LiOH delivered free acid **9** in 83% yield. Compound **9** was coupled to dipeptide **10** (derived of *N*-Boc-D-alanine and glycine methyl ester in two steps, see Supporting Information) using EDCI and HOBt. Final saponification in THF/LiOH provided the lipopeptide side chain **11b** (69% yield over two steps). Overall, **11b** was obtained in 7 linear steps and a yield of 49%.

SPPS of the second building block commenced with commercially available 2-chloro-2-trityl resin preloaded (0.4–1.0 mmol/g) with O-^{t}Bu-L-tyrosine (**12**). *N*-Fmoc protection chemistry was employed for mild, non-racemizing conditions,[20] with further reduction of the amounts of DBU (0.5%) used during deprotection.

Quantitative conversion of each individual SPPS step was controlled by cleavage of analytical amounts of product from the resin by treatment with 1% TFA followed by HPLC analysis (for HPLC chromatograms, see Figure S1). Attachment of Fmoc-L-alanine was achieved using DIC and HOBt in DMF delivering **13** (Scheme 2). Fmoc removal (**14**) with DBU and attachment of Fmoc-L-HPG with COMU/NEt_3 in DMF furnished tripeptide **15**. Removal of the Fmoc protection group (**16**) and installation of an *N-ortho*-nitrobenzenesulfonyl (nosyl) group (**17**) set the stage for selective mono *N*-methylation to **18** following Kessler's protocol.[21] Removal of the nosyl group using mercaptoethanol liberated the amine **19**, permitting installation of the lipopeptide chain **11b** directly on resin to give **20b**. Treatment of the resin with 9% TFA (v/v) in CH_2Cl_2 released the product with concomitant *O*-^{t}Bu deprotection at the tyrosine residue to give the linear arylomycin A2 precursor **3b**. While simultaneous deprotection of the serine *O*-^{t}Bu group is possible upon longer treatment with TFA to directly deliver free **3a**, this also leads to significant epimerization. The fully unprotected arylomycin A2 precursor **3a** was thus prepared by coupling of unprotected **11a** (available by TFA-mediated deprotection of **11b**, see

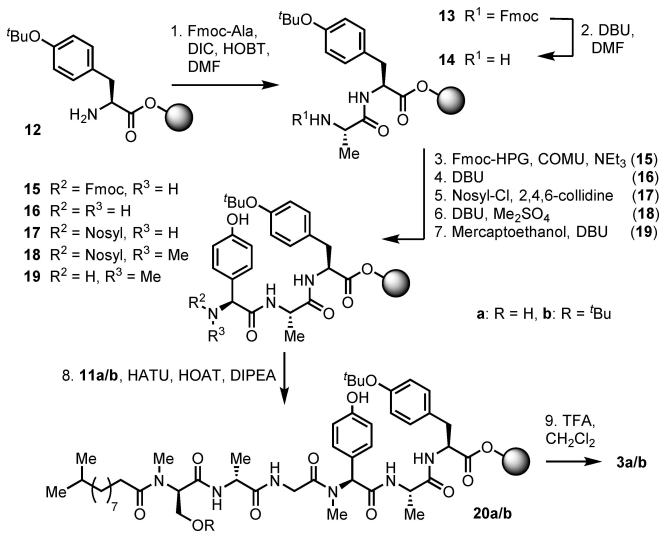

Scheme 2. Assembly of the linear arylomycin precursors **3 a/b**.

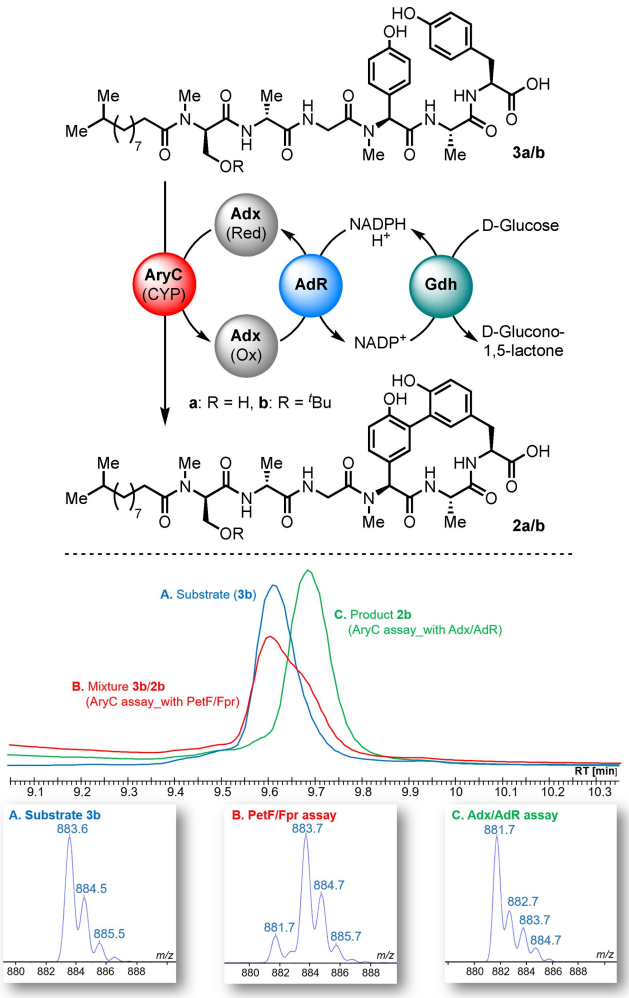

Scheme 3. Top: Biocatalytic cross-coupling of untethered, linear peptide precursors **3 a/b** to arylomycin **2 a/b** using AryC. Employed recombinant enzymes are depicted as colored spheres. Bottom: HPLC-MS analyses of the coupling reaction of **3 b** with different electron supply systems. Analyses of pure substrate (blue), reaction with Fpr/PetF (red) and Adx/AdR (green) are shown. *m/z* (substrate) = 883.6. *m/z* (product) = 881.7. For HRMS data and full HPLC-MS chromatograms, see Supporting Information.

Supporting Information) to the still resin-bound **19** to give **20a** with subsequent release from the resin.

Having precursors **3a/b** in hands, we next turned our attention to the production of recombinant AryC. The corresponding gene *aryC* was amplified by polymerase chain reaction (PCR) from genomic desoxyribonucleic acid (gDNA) of the natural arylomycin producer strain *Streptomyces roseosporus* NRRL15998 (see Supporting Information for experimental details) and cloned into expression vector pHis8-TEV (TEV = Tobacco Etch Virus nuclear-inclusion-a endopeptidase), permitting production of AryC with an *N*-terminal octa-histidine tag for downstream affinity purification. AryC was expressed in *Escherichia coli* BL21 and the purified recombinant enzyme was reconstituted with its heme-cofactor using heminchloride,[22] followed by subsequent desalting and resulting in AryC for enzymatic cross-coupling experiments, crystallization and structure determination.

Despite the expectation that AryC requires PCP-bound **3** for efficient substrate recognition - in analogy to all current examples of enzymatic glycopeptide (bio)synthesis - we first probed its activity on free substrates, initially starting with **3b**. In these assays, the redox enzyme pair Fpr/PetF,[4b] which was also produced recombinantly in *E. coli* (see Supporting Information), was applied to shuttle electrons from the primary electron source NADPH to AryC. HPLC-MS analysis suggested very low turnover, further pointing at the potential PCP-dependency of AryC. Nevertheless, small amounts of putative product **2b** were detectable by HPLC-MS. We next tested the effect of using different redox enzymes on coupling efficiency. A simple exchange of the redox system to the mammalian adrenodoxin/adrenodoxin reductase system Adx/AdR[23] indeed facilitated efficient biaryl coupling of the free acid precursor **3b** to directly deliver arylomycin **2b**, without requirement for any further activation or tethering (Scheme 3).

Identical activity was found for **3 a** to deliver arylomycin A2 (**2 a**). Furthermore, additional application of recombinant glucose dehydrogenase GdhBM3 permitted in situ recycling of $NADP^+$ from glucose.[24] Overall, AryC is thus the first cytochrome P450 enzyme installing biaryl elements into NRPS-derived peptides to function without substrate-tethering and can thus efficiently be employed in the biocatalytic synthesis of arylomycin-type antibiotics.

Owing to this unprecedented activity of AryC on untethered, free substrates, we next aimed for its structural characterization by protein crystallography. Crystals of AryC fully reconstituted with hemin diffracted to 2.5 Å and the structure was solved by molecular replacement taking advantage of the conserved core structure of P450s, despite their generally low sequence conservation (for data processing and structure refinement statistics, see Supporting Information; structure-based sequence alignment, see Figure S2). AryC shares the common, prism-like folding topology of P450s, characterized by

a large α-helical domain and a small β-sheet-rich domain, with the b-type heme cofactor sandwiched in between and deeply buried within the enzyme (Figures 2 and S3). The heme-iron is axially coordinated by the conserved, proximal Cys 355 residue, forming the iron-cysteinate bond, essential for the oxidation reaction carried out by this enzyme class. AryC shares about 35%–40% sequence identity to other available P450s structures and can be superimposed with a root mean square of 1.5–3 Å (Figure S4).

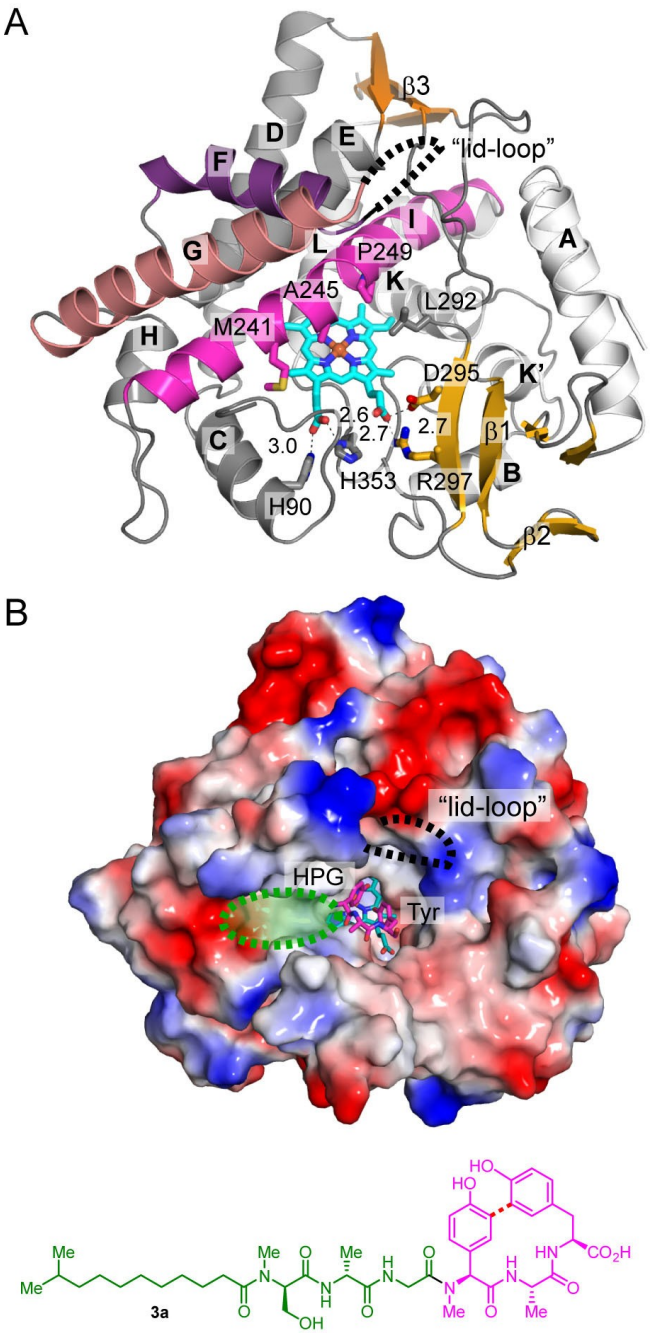

Figure 2. Structure of AryC. A) Overall folding topology of AryC displayed as ribbon. The heme and residues lining the active site are shown as stick model. Secondary structure elements are annotated as for P450s (α-helices A–L, β-sheets 1–3) and the flexible lid-loop is indicated by a dashed line. B) Amino acid charges are mapped onto surface of AryC, highlighting the hydrophobic entrance channel to the active site. Proposed model for the binding-mode of the HPG-Ala-Tyr-moiety of the substrate (pink stick model) and likely positions of the lipophilic tail (green) are highlighted. The heme at the bottom of the active site is shown as cyan stick model.

The flexible loop that connects helices F and G (resi 170–190) and usually acts as a lid to the active site entrance of P450s is not resolved in the crystal structure of AryC. This loop is commonly disordered in most of the P450 structures reported to date and can be involved in interactions with PCPs).[25] Although the PCP carrier is not required for AryC-activity in vitro, as shown above, based on structural superposition of AryC with the two available P450s in complex with their respective substrate-bound PCPs allows to identify a potential binding site for the PCP-carrier at the *N*-terminus of helix G, the interface of the *N*-terminal loop region with the *C*-terminus of helix I and/or the β1-sheet (Figure S5). Moreover, AryC contains a conserved PXXD-motif at the *N*-terminus of helix F. A PRDD motif was shown to be responsible for the interaction with the X-domain in the P450 OxyB catalyzing the first peptide cyclization step in vancomycin biosynthesis,[5] and is present in AryC, despite the NRPS lacking such an X-domain (Figure S5). The funnel-shaped channel to the catalytic center is about 22 Å long, and predominantly lined with aliphatic residues, resulting in a pronounced hydrophobic character (Figure 2, Figure S6). Substrate specificity and scope in P450s is determined by the accessibility of the catalytic heme-iron and fine-tuned by amino acid residues in helix I located above the proximal face of the heme[5b] (Figure 2A). Analysis of the sequence conservation in P450s that catalyze biaryl-formation as listed in the work by Jin et al.[18] showed the for P450s typical sequence conservation at the proximal heme-site. However, only some sequence similarities in the amino acids lining the active site at the distal heme-face, particular located at helix I, are present (Figure S7). This is not unexpected and likely due to the fact that the residues lining the active site are only responsible for optimal positioning of the substrate, but do not take part in the catalytic reaction, which is performed by the heme-iron. Thus, the amino acid residues forming the active site are adapted to substrate scope of a particular biaryl-formation catalyzing P450, albeit the substrate scope of P450s is generally very broad. Figures 2B and S8 show a model for the possible binding mode of the HPG-Ala-Tyr-moiety of the substrate **3** to AryC, with the phenol rings of the HPG and Tyr-residues positioned over the heme face. The lipophilic tail of the substrate could thereby slot in the hydrophobic cavity (highlighted in green). This, in combination with the overall hydrophobic character of the entrance tunnel, most likely explains the ability of AryC to accept free lipopeptide substrates **3**, without additional PCP tethering. This assumption is further corroborated by the inability of AryC to convert substrate analogs of **3** devoid of the lipopeptide side-chain as well as PCP-bound precursors in our hands. The interaction with the lipopeptide side-chain along with the available space of the hydrophobic funnel-shaped entrance channel to the AryC active site also explains the ability of this enzyme to even accept the unnatural, protected *O*-^{t}Bu-D-Ser synthetic analog **3b**.

Taken together, we have developed a convergent synthesis of arylomycin-type linear lipopeptide precursors **3** by combining liquid- and solid-phase peptide synthesis. Probing of the catalytic activity of AryC – the cytochrome P450 catalyzing biaryl formation in arylomycin biosynthesis – with **3** uncovered its unprecedented ability to accept these untethered, free precursors as substrates. Enzymatic cross-coupling by AryC thus for the first time establishes the biaryl structural element without the requirement of attaching precursor peptide substrates to PCP- or PCP-X interaction partners, an important precondition for developing chemo-enzymatic approaches to BCPs. Moreover, the here provided structural and functional data could aid to modulate and adapt the substrate scope of AryC by site-directed mutagenesis of residues positioned around the heme-face and lining the substrate channel. This sets the stage for future biocatalytic application of AryC in the synthesis of arylomycin analogs.

X-ray crystallography

Crystallographic data (atomic coordinates and structure factors) of AryC have been deposited in the Protein Data Bank (PDB) with accession code 7AYX. These data are provided free of charge by the PDB and can be accessed at https://www.ebi.ac.uk/pdbe/entry/pdb/7ayx.

Acknowledgements

This project was generously funded by the German Research Foundation (DFG, GU 1233/1-1, SCHN 1273/6-1, Center for Integrated Protein Science Munich, CIPSM; EXC114). Shuangjie Shu, Hanna Hong and Tobias M. Milzarek thank the Chinese Scholarship Council (CSC), the Evonik Foundation, and the Stiftung der Deutschen Wirtschaft, respectively, for their PhD scholarships. We thank Prof. Rita Bernhardt (Saarland University, Saarbrücken) and Prof. Frank Schulz (Ruhr University Bochum) for kindly providing plasmid templates for amplification of *adr*/*adx* (pBAR1607/pKKAdx) and *gdh* (pACYCDuet-1::*gdh*-BM3), respectively. Open Access funding enabled and organized by Projekt DEAL.

Conflict of Interest

The authors declare no conflict of interest.

Keywords: arylomycin · biaryl coupling · chemo-enzymatic synthesis · crystal structure · cytochrome P450

[1] M. H. McCormick, W. M. Stark, G. E. Pittenger, R. C. Pittenger, J. M. McGuire, *Antibiot. Annu.* **1955**, *56*, 606–611.
[2] a) R. D. Suessmuth, A. Mainz, *Angew. Chem. Int. Ed. Engl.* **2017**, *56*, 3770–3821; *Angew. Chem.* **2017**, *129*, 3824–3878; b) B. K. Hubbard, C. T. Walsh, *Angew. Chem. Int. Ed. Engl.* **2003**, *42*, 730–765; *Angew. Chem.* **2003**, *115*, 752–789; c) R. D. Suessmuth, W. Wohlleben, *Appl. Microbiol. Biotechnol.* **2004**, *63*, 344–350.
[3] a) D. Bischoff, S. Pelzer, A. Höltzel, G. J. Nicholson, S. Stockert, W. Wohlleben, G. Jung, R. D. Suessmuth, *Angew. Chem. Int. Ed.* **2001**, *40*, 1693–1696; *Angew. Chem.* **2001**, *113*, 1736–1739; b) D. Bischoff, S. Pelzer, B. Bister, G. J. Nicholson, S. Stockert, M. Schirle, W. Wohlleben, G. Jung, R. D. Suessmuth, *Angew. Chem. Int. Ed.* **2001**, *40*, 4688–4691; *Angew. Chem.* **2001**, *113*, 4824–4827; c) S. Pelzer, R. D. Suessmuth, D. Heckmann, J. Recktenwald, P. Huber, G. Jung, W. Wohlleben, *Antimicrob. Agents Chemother.* **1999**, *43*, 1565–1573; d) E. Stegmann, S. Pelzer, D. Bischoff, O. Puk, S. Stockert, D. Butz, K. Zerbe, J. Robinson, R. D. Suessmuth, W. Wohlleben, *J. Biotechnol.* **2006**, *124*, 640–653; e) J. Recktenwald, R. Shawky, O. Puk, F. Pfennig, U. Keller, W. Wohlleben, S. Pelzer, *Microbiology* **2002**, *148*, 1105–1118; f) D. Bischoff, B. Bister, M. Bertazzo, V. Pfeifer, E. Stegmann, G. J. Nicholson, S. Keller, S. Pelzer, W. Wohlleben, R. D. Suessmuth, *ChemBioChem* **2005**, *6*, 267–272.
[4] a) K. Zerbe, K. Woithe, D. B. Li, F. Vitali, L. Bigler, J. A. Robinson, *Angew. Chem. Int. Ed.* **2004**, *43*, 6709–6713; *Angew. Chem.* **2004**, *116*, 6877–6881; b) K. Woithe, N. Geib, K. Zerbe, D. B. Li, M. Heck, S. Fournier-Rousset, O. Meyer, F. Vitali, N. Matoba, K. Abou-Hadeed, J. A. Robinson, *J. Am. Chem. Soc.* **2007**, *129*, 6887–6895; c) K. Woithe, N. Geib, O. Meyer, T. Wortz, K. Zerbe, J. A. Robinson, *Org. Biomol. Chem.* **2008**, *6*, 2861–2867; d) N. Geib, K. Woithe, K. Zerbe, D. B. Li, J. A. Robinson, *Bioorg. Med. Chem. Lett.* **2008**, *18*, 3081–3084; e) D. B. Li, K. Woithe, N. Geib, K. Abou-Hadeed, K. Zerbe, J. A. Robinson, *Methods Enzymol.* **2009**, *458*, 487–509; f) D. B. Li, J. A. Robinson, *Org. Biomol. Chem.* **2005**, *3*, 1233–1239.
[5] a) K. Haslinger, M. Peschke, C. Brieke, E. Maximowitsch, M. J. Cryle, *Nature* **2015**, *521*, 105–109; b) M. Peschke, M. Gonsior, R. D. Suessmuth, M. J. Cryle, *Curr. Opin. Struct. Biol.* **2016**, *41*, 46–53.
[6] a) C. C. Forneris, M. R. Seyedsayamdost, *Angew. Chem. Int. Ed.* **2018**, *37*, 8048–8052; *Angew. Chem.* **2018**, *130*, 8180–8184; b) J. Tailhades, Y. Zhao, M. Schoppet, A. Greule, R. J. A. Goode, R. B. Schittenhelm, J. J. De Voss, M. J. Cryle, *Org. Lett.* **2019**, *21*, 8635–8640; c) Y. Zhao, R. J. A. Goode, R. B. Schittenhelm, J. Tailhades, M. J. Cryle, *J. Org. Chem.* **2020**, *85*, 1537–1547; d) J. Tailhades, Y. Zhao, Y. T. C. Ho, A. Greule, I. Ahmed, M. Schoppet, K. Kulkarni, R. J. A. Goode, R. B. Schittenhelm, J. J. De Voss, M. J. Cryle, *Angew. Chem. Int. Ed.* **2020**, *59*, 10899–10903; *Angew. Chem.* **2020**, *132*, 10991–10995.
[7] Y. Zhao, Y. T. C. Ho, J. Tailhades, M. J. Cryle, *ChemBioChem* **2021**, *22*, 43–51.
[8] J. Schimana, K. Gebhardt, A. Höltzel, D. G. Schmid, R. Suessmuth, J. Müller, R. Pukall, H.-P- Fiedler, *J. Antibiot.* **2002**, *55*, 565–570.
[9] a) P. Kulanthaivel, A. J. Kreuzman, M. A. Strege, M. D. Belvo, T. A. Smitka, M. Clemens, J. R. Swartling, K. L. Minton, F. Zheng, E. L. Angleton, D. Mullen, L. N. Jungheim, V. J. Klimkowski, T. I. Nicas, R. C. Thompson, S.-B-Peng, *J. Biol. Chem.* **2004**, *279*, 36250–36258; b) M. Paetzel, J. J. Goodall, M. Kania, R. E. Dalbey, M. G. P. Page, *J. Biol. Chem.* **2004**, *279*, 30781–30790; c) C. Luo, P. Roussel, J. Dreier, M. G. P. Page, *Biochemistry* **2009**, *48*, 38, 8976–8984; d) P. A. Smith, F. E. Romesberg, *Antimicrob. Agents Chemother.* **2012**, *56*, 5054–5060; e) S. Walsh, D. S. Peters, P. A. Smith, A. Craney, M. M. Dix, B. F. Cravatt, F. E. Romesberg, *Antimicrob. Agents Chemother.* **2019**, *63*, 1–13.
[10] a) T. C. Roberts, P. A. Smith, R. T. Cirz, F. E. Romesberg, *J. Am. Chem. Soc.* **2007**, *129*, 15830–15838; b) J. Dufour, L. Neuville, J. Zhu, *Synlett* **2008**, 2355–2359; c) J. Dufour, L. Neuville, J. Zhu, *Chemistry* **2010**, *16*, 10523–10534; d) J. Liu, C. Luo, P. A. Smith, J. K. Chin, M. G. P. Page, *J. Am. Chem. Soc.* **2011**, *133*, 17869–17877.
[11] a) T. C. Roberts, M. A. Schallenberger, J. Liu, P. A. Smith, F. E. Romesberg, *J. Med. Chem.* **2011**, *54*, 4954–4963; b) J. Liu, P. A. Smith, D. B. Steed, F. E. Romesberg, *Bioorg. Med. Chem. Lett.* **2013**, *23*, 5654–5659.
[12] P. A. Smith, M. F. T. Koehler, H. S. Girgis, D. Yan, Y. Chen, Y. Chen, J. J. Crawford, M. R. Durk, R. I. Higuchi, J. Kang, J. Murray, P. Paraselli, S. Park, W. Phung, J. G. Quinn, T. C. Roberts, L. Rougé, J. B. Schwarz, E. Skippington, J. Wai, M. Xu, Z. Yu, H. Zhang, M.-W. Tan, C. E. Heise, *Nature* **2018**, *561*, 189–194.
[13] N.-K. Lim, X. Linghu, N. Wong, H. Zhang, C. G. Sowell, F. Gosselin, *Org. Lett.* **2019**, *21*, 147–151.
[14] N. Wong, F. Petronijević, A. Y. Hong, X. Linghu, S. M. Kelly, H. Hou, T. Cravillion, N.-K. Lim, S. J. Robinson, C. Han, C. Molinaro, C. G. Sowell, F. Gosselin, *Org. Lett.* **2019**, *21*, 9099–9103.
[15] D. S. Peters, F. E. Romesberg, P. S. Baran, *J. Am. Chem. Soc.* **2018**, *140*, 2072–2075.
[16] M. Ben-Lulu, E. Gaster, A. Libman, D. Pappo, *Angew. Chem. Int. Ed. Engl.* **2020**, *59*, 4835–4839; *Angew. Chem.* **2020**, *132*, 4865–4869.

[17] W. T. Liu, R. D. Kersten, Y.-L. Yang, B. S. Moore, P. C. Dorrestein, *J. Am. Chem. Soc.* **2011**, *133*, 18010–18013.
[18] X. Jin, M. Rao, W. Wei, M. Ge, J. Liu, D. Chen, Y. Liang, *Biotechnol. Lett.* **2012**, *34*, 2283–2289.
[19] G. Cahiez, C. Chaboche, M. Jézéquel, *Tetrahedron* **2000**, *56*, 2733–2737.
[20] C. Brieke, M. J. A. Cryle, *Org. Lett.* **2014**, *16*, 2454–2457.
[21] E. Biron, J. Chatterjee, H. Kessler, *J. Peptide Sci.* **2006**, *12*, 213–219.
[22] S. Schneider, K. H. Sharp, P. D. Barker, M. Paoli, *J. Biol. Chem.* **2006**, *281*, 32606–32610.
[23] K. M. Ewen, M. Ringle, R. Bernhardt, *IUBMB Life* **2012**, *64*, 506–512.
[24] A. Weckbecker, W. Hummel, *Glucose dehydrogenase for the regeneration of NADPH and NADH in Microbial Enzymes and Biotransformations* (Ed.: Barredo, J. L.), Humana Press, Totowa, NJ, **2005**, pp. 225–238.
[25] a) M. J. Cryle, I. Schlichting, *PNAS* **2008**, *105*, 15696–15701; b) K. Haslinger, C. Brieke, S. Uhlmann, L. Sieverling, R. D. Süssmuth, M. J. Cryle, *Angew. Chem. Int. Ed. Engl.* **2014**, *53*, 8518–8522.

Manuscript received: September 16, 2021
Accepted manuscript online: November 2, 2021
Version of record online: November 26, 2021